



## Effect of field-annealing on magnetostriction and tunneling magnetoresistance of Co/AIO<sub>x</sub>/Co/IrMn junctions

Yuan-Tsung Chen<sup>a,\*</sup>, Jiun-Yi Tseng<sup>b</sup>, C.C. Chang<sup>a</sup>, W.C. Liu<sup>a</sup>, Jason Shian-Ching Jang<sup>c</sup>

<sup>a</sup> Department of Materials Science and Engineering, I-Shou University, Kaohsiung 840, Taiwan, ROC

<sup>b</sup> Institute of Physics, Academia Sinica, Taipei 11529, Taiwan, ROC

<sup>c</sup> Department of Mechanical Engineering, Institute of Materials Science & Engineering, National Central University, Chung-Li 320, Taiwan, ROC

### ARTICLE INFO

#### Article history:

Received 7 August 2009

Accepted 13 September 2009

Available online 19 September 2009

#### PACS:

75.30.Et

75.60.Nt

75.70.-i

#### Keywords:

Magnetic films and multilayers

Magnetoresistance

Magnetostriction ( $\lambda_s$ )

Field-annealing effect

Oxidation

### ABSTRACT

The magnetostriction ( $\lambda_s$ ) and tunneling magnetoresistance (TMR) of two Co/AIO<sub>x</sub>/Co/IrMn MTJ systems that were deposited on Si(100) and glass substrate were examined at RT and field-annealing with various thicknesses of AIO<sub>x</sub>. One structure was a Si(100)/Ta/Co/AIO<sub>x</sub>/Co/IrMn/Ta system, and the other was a glass/Co/AIO<sub>x</sub>/Co/IrMn system. The experimental results reveal that, in the Si(100)/Ta/Co/AIO<sub>x</sub>/Co/IrMn/Ta system, the ratio of TMR is maximal under the field-annealing condition, and is optimal at an AIO<sub>x</sub> thickness of 26 Å as well as in the RT condition. EDS analysis demonstrates that, these results are related to the distribution of Co and O atoms, because the oxidation of AIO<sub>x</sub> is most extensive at a thickness of 26 Å. In the glass/Co/AIO<sub>x</sub>/Co/IrMn system,  $\lambda_s$  does not significantly vary under the RT condition; however,  $\lambda_s$  is maximized (−20 ppm) by field-annealing at an AIO<sub>x</sub> thickness of 17 Å. The abundance of Co and O in the system dominates the behavior of  $\lambda_s$ , according to EDS analysis. Finally, the minimum value of  $\lambda_s$  and the maximum ratio of TMR are −8 ppm and 60%, respectively, at an AIO<sub>x</sub> thickness of 26 Å under the field-annealing condition.

© 2009 Elsevier B.V. All rights reserved.

### 1. Introduction

Favorable combinations of characteristics of magnetic tunneling junctions (MTJs), including low magnetostriction ( $\lambda_s$ ) and high tunneling magnetoresistance (TMR), are crucial to optimizing the performance of an MTJ device in high-temperature environments. Tolerance to high temperatures is important in read head sensors and magnetoresistance random access memory (MRAM) [1–3].

Generally, the AIO<sub>x</sub> layer, after field-annealing treatment, of an MTJ, which serves as a barrier to tunneling, increases the TMR value [4,5]. The TMR ratio of AIO<sub>x</sub>-based MTJ has been found to increase with annealing temperature ( $T_A$ ) up to 265 °C [6]. However, Mn atoms diffuse toward the tunneling barrier ( $T_A > 350$  °C), reducing the TMR value [7].

Another important parameter,  $\lambda_s$ , is also important to MRAM applications. The signal is disturbed according to large  $\lambda_s$  when the device is in the process of reading/writing. Recently,  $\lambda_s$  and TMR of the AIO<sub>x</sub>-based MTJ have been studied [8–11], but much remains to be explored. Chen et al. found that the maximum TMR and minimum  $\lambda_s$  were 36% and −15 ppm, respectively, in a Co/AIO<sub>x</sub>/Co/IrMn junction at RT [11]. Accordingly, this investiga-

tion focuses on the values of TMR and  $\lambda_s$  in the field-annealed Co/AIO<sub>x</sub>/Co/IrMn junction. Recent results show that field-annealing treatment can improve the magnetic properties of Co/AIO<sub>x</sub>/Co/IrMn junctions. Additionally, the TEM results indicate that the Co/AIO<sub>x</sub> and AIO<sub>x</sub>/Co interfaces are smooth, increasing higher the TMR values [12,13]. To determine how varying AIO<sub>x</sub> thickness ( $\delta t_0$ ) varies the chemical composition of the AIO<sub>x</sub> barrier, a cross-sectional high-resolution transmission electron microscope (HRTEM) with the ability to obtain a nanoprobe energy dispersive spectrum (EDS) was utilized to analyze the distributions of Co, Al, O, Ir and Mn concentrations on the cross-section across the AIO<sub>x</sub> layers.

### 2. Experimental details

A cross-strip MTJ with the structure Si(100)/Ta(30 Å)/Co(75 Å)/AIO<sub>x</sub>( $\delta t_0$ )/Co(75 Å)/IrMn(90 Å)/Ta(100 Å) was deposited onto a Si(100) substrate by magnetron sputtering, where  $\delta t_0 = 12, 17, 22, 26, \text{ and } 30$  Å. The IrMn layer was deposited using an alloy target with a composition of 20 at.% Ir and 80 at.% Mn. The TMR and  $\lambda_s$  of two sets of MTJ specimens, prepared using different treatments during deposition, were studied. The treatments were as follows: (a) substrate temperature ( $T_s$ ) maintained at RT an in-plane deposition field,  $h = 500$  Oe, and (b)  $T_s = \text{RT}$  with an in-plane deposition field,  $h = 500$  Oe during deposition, with post-deposition annealing in the field at  $T_A = 250$  °C for 1 h, before the samples were field-cooled to RT. The typical pressure of the base chamber was less than  $1 \times 10^{-7}$  Torr, and the pressure of the Ar working chamber was maintained at  $5 \times 10^{-3}$  Torr. Furthermore, the  $\lambda_s$  of the glass/Co(75 Å)/AIO<sub>x</sub>( $\delta t_0$ )/Co(75 Å)/IrMn(90 Å) MTJ, where  $\delta t_0 = 12, 17, 22, 26, \text{ and } 30$  Å, was also measured using the optical-cantilever method following two treatments [14,15]. To increase the sensitivity and reduce the substrate effect, a glass

\* Corresponding author. Tel.: +886 765 777 11; fax: +886 765 784 44.  
E-mail address: [ytchen@isu.edu.tw](mailto:ytchen@isu.edu.tw) (Y.-T. Chen).

substrate was used in the measurement of  $\lambda_s$ . The TMR ratio of the MTJ device that was deposited on the Si substrate was found, and this device was determined to be compatible with the semiconductor process.

To prepare an  $\text{AlO}_x$  barrier, Al was initially deposited on the bottom FM electrode (Co layer), and the  $\text{AlO}_x$  barrier layer was then formed by plasma oxidation in an oxidizing atmosphere of a mixture of Ar/ $\text{O}_2$  in the ratio 9:16. The plasma oxidation time was varied from 30 to 70 s and the initial thickness of the Al layer was thus increased from 12 to 30 Å. Each MTJ was fabricated by the cross-strip method with a cross-sectional junction area of 0.0225 mm<sup>2</sup>. The conventional four-point technique is adopted in a typical measurement of TMR ratio. To understand how varying  $\delta t_0$  alters the chemical composition of the  $\text{AlO}_x$  barrier, a cross-sectional HRTEM with EDS capability was employed to analyze the Co, Al, O, Ir and Mn concentrations ( $x_{\text{Co}}$ ,  $x_{\text{Al}}$ ,  $x_{\text{O}}$ ,  $x_{\text{Ir}}$ , and  $x_{\text{Mn}}$ ) across each  $\text{AlO}_x$  layer.

### 3. Results and discussion

Fig. 1 presents a typical cross-sectional HRTEM image of a  $\text{Co}(75 \text{ \AA})/\text{AlO}_x(26 \text{ \AA})/\text{Co}(75 \text{ \AA})$  field-annealed MTJ. After field-annealing at 250 °C, the laminated structure of  $\text{Co}(75 \text{ \AA})/\text{AlO}_x(26 \text{ \AA})/\text{Co}(75 \text{ \AA})$  MTJ had the following features, which may explain the general increase in TMR (Fig. 2) and the decline in  $\lambda_s$  (Fig. 3). First, the crystallinity of the Co layers on both sides improved as the degree of texturing after field-annealing increased, potentially increasing the spin polarization  $P$  of each Co layer. Second, the  $\text{Co}/\text{AlO}_x$  and  $\text{AlO}_x/\text{Co}$  interfaces had been modified to make them smoother with low waviness, due to field-annealing. Third, the  $\text{AlO}_x$  tunneling remained amorphous following field-annealing.

Fig. 2 plots the TMR ratio versus  $\delta t_0$  at RT following field-annealing at 250 °C. Before annealing at RT, as in our earlier investigation [11], the TMR ratio was initially low, increased from 21% to 36%, and finally declined to 24%. After field-annealing at 250 °C, the TMR ratio increased from 27% to 60% and then eventually fell back to 52%. In the range of  $\delta t_0$  from 12 to 22 Å, the TMR values of

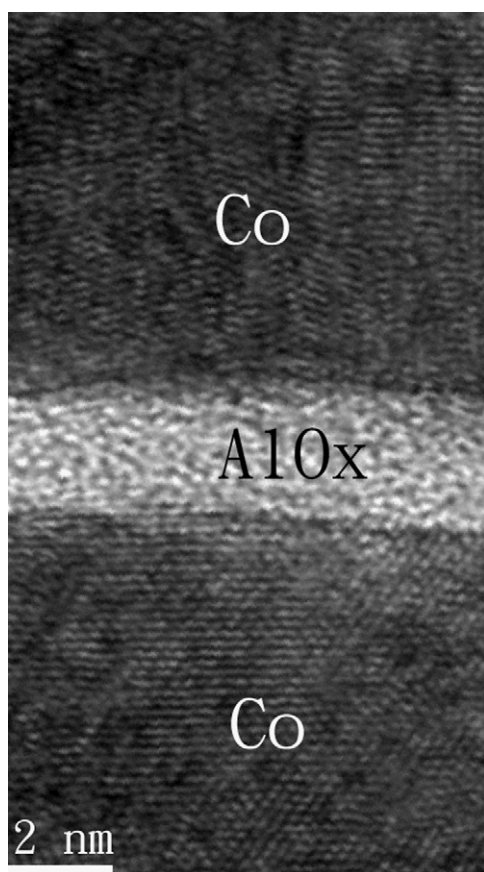


Fig. 1. Cross-sectional HR-STEM image of  $\text{Co}(75 \text{ \AA})/\text{AlO}_x(26 \text{ \AA})/\text{Co}(75 \text{ \AA})$  field-annealed MTJ.

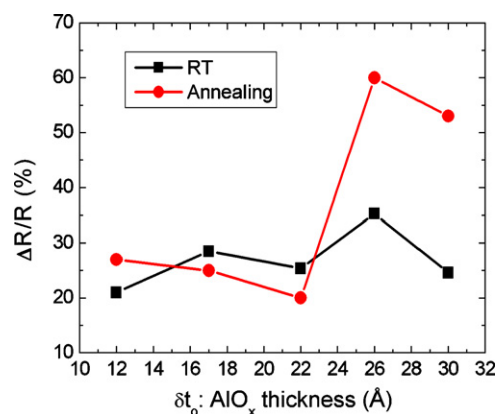


Fig. 2. TMR ratio ( $\Delta R/R$ ) versus thickness ( $\delta t_0$ ) of  $\text{AlO}_x$  layer following RT and field-annealing at 250 °C.

RT and field-annealed at 250 °C were approximately equal. In both cases, the TMR ratio was small, but it exceeded 20% in this range of  $\delta t_0$ . This finding may be attributed to the presence of pin-holes, which cause the spin scanning effect [16]. In contrast, the MTJ after field-annealing at 250 °C exhibited a much larger TMR ratio than the RT MTJ, reaching a maximum TMR ratio of 60% at  $\delta t_0 = 26 \text{ \AA}$ . This result may follow from the improvement in the interface roughness and the Co crystallinity due to field-annealing [17]. Another possible cause is the polarization and depolarization of spin tunneling in the oxidation plasma process [11]. Briefly, if  $\delta t_0$  is too small (such as  $\delta t_0 = 12 \text{ \AA}$ ), then the Co bottom electrode may be over oxidized, causing the free Co layer to be less polarized, resulting in a lower spin-tunneling current. If  $\delta t_0$  is too high (such as  $\delta t_0 = 30 \text{ \AA}$ ), then the spin-polarized current may be depolarized excessively in the spin-tunneling process. This depolarization effect would also reduce TMR value. Moreover, the phenomenon of increasing- and -decreasing TMR ratio upon the RT and field-annealing at 250 °C of MTJs, shown in Fig. 2, may reveal that the spin-tunneling effect is also sensitive to the physical and chemical conditions of the two interfaces of the MTJ junction [18]. The oscillatory profile of the TMR ratio results from the inter-layer coupling effect, implying that ferromagnetic electrode coupling obeys Bruno's reflection model [13].

Fig. 3 plots the dependence of magnetostriction on the tunneling barrier  $\text{AlO}_x$  in the  $\text{glass}/\text{Co}(75 \text{ \AA})/\text{AlO}_x(\delta t_0)/\text{Co}(75 \text{ \AA})/\text{IrMn}(90 \text{ \AA})$  MTJ following RT and field-annealing at 250 °C. The figure also presents the concave-up feature, with the most negative  $\lambda_s$  value at  $\delta t_0 = 17 \text{ \AA}$  [10]. The  $\lambda_s$  of the MTJ following field-annealing at 250 °C is generally in the range of  $-20$  to  $-8$  ppm, which is lower

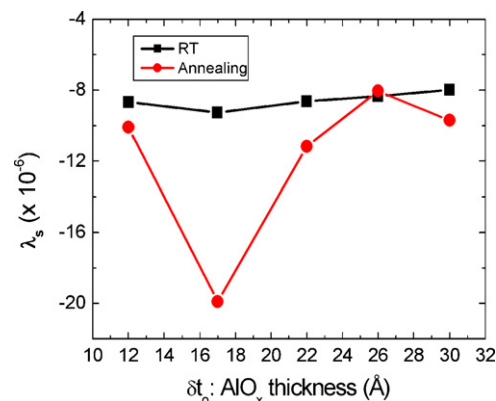
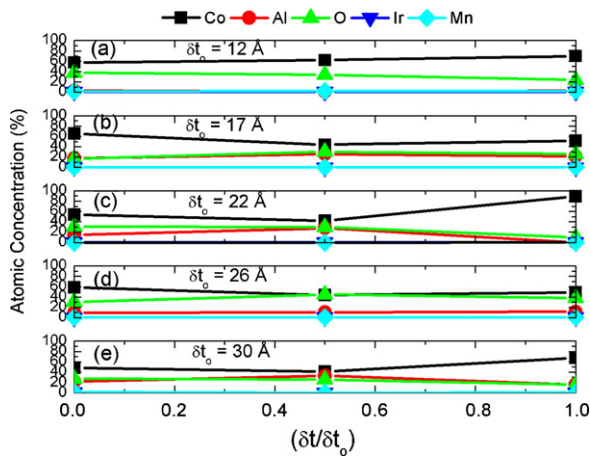


Fig. 3. Magnetostriction  $\lambda_s$  of  $\text{glass}/\text{Co}(75 \text{ \AA})/\text{AlO}_x(\delta t_0)/\text{Co}(75 \text{ \AA})/\text{IrMn}(90 \text{ \AA})$  junction following RT and field-annealing at 250 °C.



**Fig. 4.** Atomic concentrations of Co, Al, O, Ir and Mn analyzed across the  $\text{AlO}_x$  thickness in the  $\text{Co}(75 \text{ \AA})/\text{AlO}_x(\delta t_0)/\text{Co}(75 \text{ \AA})/\text{IrMn}(90 \text{ \AA})$  field-annealed junction, where  $\delta t_0 =$  (a) 12 Å, (b) 17 Å, (c) 22 Å, (d) 26 Å, and (e) 30 Å.

than that of the RT MTJ, because field-annealing treatment leads to inter-diffusion in the MTJ. Additionally, the  $\lambda_s$  value of an MTJ junction can be controlled in two ways [10]. First, the  $\lambda_s$  of an MTJ can be macro-turned by adjusting the thickness of the two ferromagnetic Co electrodes. Second,  $\lambda_s$  can be micro-tuned by varying  $\delta t_0$ , causing  $\lambda_s$  to exhibit a concave-up characteristic.

Fig. 4 plots atomic concentrations ( $x_{\text{Co}}$ ,  $x_{\text{Al}}$ ,  $x_{\text{O}}$ ,  $x_{\text{Ir}}$ , and  $x_{\text{Mn}}$ ) as functions of the normalized ( $\delta t/\delta t_0$ ) position in the  $\text{AlO}_x$  layer, obtained by EDS analysis across the  $\text{AlO}_x$  thickness of the MTJ following field-annealing at 250 °C, respectively. According to a previous investigation [19], an MTJ has two  $\lambda_s$  zones: zone (I) is an O-rich CoO film; zone (II) is a Co-rich CoO film. Variations in the thickness of the  $\text{AlO}_x$  layer, which acts as a diffusion barrier, cause variation in the distributions of concentrations of O and Co during field-annealing. As the  $\delta t_0$  thickness increases from 12 to 17 Å,  $x_{\text{O}}$  decreases from 38% to 16% and  $x_{\text{Co}}$  increases from 57% to 66%. Zone II therefore becomes thicker than zone I, yielding a more negative  $\lambda_s$  value after field-annealing [14]. Conversely, as the thickness  $\delta t_0$  increases from 17 to 22 Å,  $x_{\text{O}}$  increases from 16% to 30% and  $x_{\text{Co}}$  after field-annealing decreases from 66% to 54%. This result indicates that the O-rich effect dominates the  $\lambda_s$  behavior, which is more positive in zone (I) in this situation. As the thickness  $\delta t_0$  increases from 22 to 26 Å,  $x_{\text{O}}$  decreases from 30% to 26% and  $x_{\text{Co}}$  following field-annealing increases from 54% to 59%, suggesting that  $\lambda_s$  is more positive in zone (II) because of the relative abundance of Co. Finally, as the thickness  $\delta t_0$  increases from 26 to 30 Å,  $x_{\text{O}}$  increases from 26% to 28% and  $x_{\text{Co}}$  after field-annealing decreases from 59% to 48%. Zone (I) returns to being O-rich, such that  $\lambda_s$  becomes more negative again. The EDS results demonstrate that the  $\lambda_s$  of field-annealed treated samples tends to be more negative than that of RT samples, potentially revealing that field-annealing at 250 °C may induce the Co-rich inter-diffusion effect. Based on the above mechanisms,  $\lambda_s$  is consistent with the EDS results, as displayed in Fig. 3.

With respect to the consistency between EDS results and TMR ratio (Fig. 2), this investigation focused on the EDS results obtained from the middle of each  $\text{AlO}_x$  tunneling layer. Fig. 5 plots the atomic concentrations of Co and O. In this figure, the O concentration increases slowly and the Co concentration declines as the  $\delta t_0$  thickness increases from 12 to 30 Å. Fig. 2 plots the TMR ratio, and suggests that the barrier thickness that optimizes the TMR ratio is 26 Å. This result is attributable to the under-oxidation in the  $\text{AlO}_x$  oxidation process. As the thickness  $\delta t_0$  is increased from 12 to 22 Å, the Co and Al atoms compete to forming an oxidized compound in the  $\text{AlO}_x$  barrier layer. A very high Co concentration can lead to the formation of a magnetic dead layer, such as  $\text{CoO}$  or  $\text{Co}_3\text{O}_4$ ,

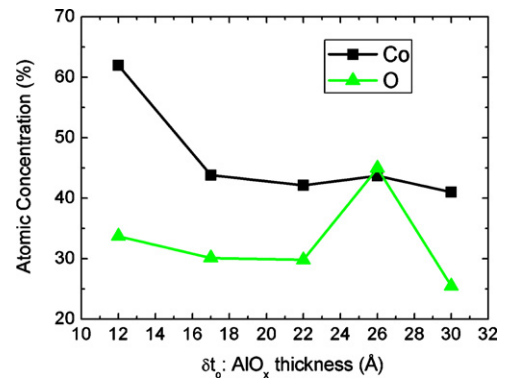


**Fig. 5.** Atomic concentrations of Co and O analyzed across  $\text{AlO}_x$  thickness in the middle of each field-annealed junction.

which is known to increase the probability of spin-flip scattering, which can reduce the spin polarization of the Co electrode [20]. In under-oxidized barriers, residual paramagnetic Al can depolarize and scatter spin-tunneling electrons, reducing the TMR ratio [21]. The optimal TMR ratio is obtained at when the  $\text{AlO}_x$  barrier layer is 26 Å thick. According to one study [12], a field-annealing of an MTJ can improve interfacial roughness, reduce the number of defects in the barrier layer and reduce the effective barrier width ( $S$ ), according to the Simmons formula. Finally, as the barrier thickness increases to 30 Å, under-oxidation associated with lower O oxidation may result in lower TMR ratio. Briefly, the 26 Å optimal  $\text{AlO}_x$  barrier thickness can be considered as a reference by which other MTJ samples can be regarded as under-oxidized.

#### 4. Conclusions

In summary, the magnetostriction ( $\lambda_s$ ) and tunneling magnetoresistance (TMR) of two MTJ systems were studied at RT and with field-annealing treatment. Field-annealing treatment was found to induce inter-diffusion of mainly Co and O, smoothing the  $\text{Co}/\text{AlO}_x$  and  $\text{AlO}_x/\text{Co}$  interfaces. This fact was verified by cross-sectional HRTEM. The optimal parameters for MTJ systems herein study were an  $\text{AlO}_x$  thickness of 26 Å, a maximum TMR of 60%, and a minimum  $\lambda_s$  of  $-8$  ppm.

#### Acknowledgements

The authors would like to thank the National Science Council of the Republic of China and I-Shou University for financially supporting this research under Contract No. NSC97-2112-M-214-001-MY3 and ISU98-S-02.

#### References

- [1] S.S.P. Parkin, C. Kaiser, A. Panchula, P.M. Rice, B. Hughes, M. Samant, S.-H. Yang, *Nat. Mater.* 3 (2004) 862.
- [2] S. Yuasa, A. Fukushima, H. Kubota, Y. Suzuki, K. Ando, *Appl. Phys. Lett.* 89 (2006) 042505.
- [3] F.F. Li, R. Sharif, L.X. Jiang, X.Q. Zhang, X.F. Han, Y. Wang, Z. Zhang, *J. Appl. Phys.* 98 (2005) 113710.
- [4] B. You, W. Sheng, L. Sun, W. Zhang, J. Du, M. Lu, H. Zhai, A. Hu, Q. Xu, Y. Wang, Z. Zhang, *J. Phys. D* 36 (2003) 2313.
- [5] D.M. Jeon, J.W. Park, D.H. Lee, S.Y. Yoon, D.H. Yoon, S.J. Suh, *J. Magn. Magn. Mater.* 272 (2004) 1956.
- [6] K.M. Wu, C.H. Huang, S.C. Lin, M.J. Ker, M.J. Tsai, J.C. Wu, L. Horng, *Phys. Status Solidi (a)* 204 (2007) 3934.
- [7] Y. Fukumoto, K.I. Shimura, A. Kamijo, S. Tahara, *Appl. Phys. Lett.* 84 (2004) 223.
- [8] N.D. Hughes, R.J. Hicken, *J. Phys. D* 35 (2002) 3153.
- [9] K.S. Yoon, J.H. Koo, Y.H. Do, K.W. Kim, C.O. Kim, J.P. Hong, *J. Magn. Magn. Mater.* 285 (2005) 125.
- [10] Y.T. Chen, S.U. Jen, Y.D. Yao, J.M. Wu, A.C. Sun, *Appl. Phys. Lett.* 88 (2006) 222509.
- [11] Y.T. Chen, S.U. Jen, Y.D. Yao, S.R. Jian, *IEEE Trans. Magn.* 44 (2008) 2592.

- [12] D.M. Jeon, J.W. Park, D.H. Lee, S.Y. Yoon, D.H. Yoon, S.J. Suh, J. Magn. Mater. 272–276 (2004) 1956.
- [13] E. Makino, S. Ishii, M. Syoji, A. Furukawa, M. Hosomi, A. Matuzono, J. Appl. Phys. 89 (2001) 7619.
- [14] S.U. Jen, T.C. Wu, C.C. Lin, K.H. Chang, Solid State Commun. 132 (2004) 259.
- [15] S.U. Jen, C.C. Lin, Thin Solid Films 471 (2005) 218.
- [16] J. Wang, Y. Liu, P.P. Freitas, E. Snoeck, J.L. Martins, J. Appl. Phys. 93 (2003) 8367.
- [17] Y. Jang, C. Nam, K.-S. Lee, B.K. Cho, Y.J. Cho, K.-S. Kim, K.W. Kim, Appl. Phys. Lett. 88 (2006) 182508.
- [18] T. Moriyama, C. Ni, W.G. Wang, X. Zhang, J.Q. Xiao, Appl. Phys. Lett. 88 (2006) 222503.
- [19] Y.T. Chen, S.U. Jen, Y.D. Yao, J.M. Wu, C.C. Lee, A.C. Sun, IEEE Trans. Magn. 42 (2006) 278.
- [20] S.H. Kim, B.S. Chun, Y.K. Kim, S.R. Lee, Metals Mater. Int. 9 (2003) 57.
- [21] T. Mitsuzuka, K. Matsuda, A. Kamijo, H. Tsuge, J. Appl. Phys. 85 (1999) 5807.